Modelling and Simulation of Magnetic Fields in the Vicinity of High Voltage Transmission Line

Romaric Adegbola
Electrical Engineering Department
University of Abomey-Calavi
Abomey-Calavi, Benin
adegbola_romaric@yahoo.fr

François Xavier Fifatin
Electrical Engineering Department
University of Abomey-Calavi
Abomey-Calavi, Benin
fifatinf@gmail.com

Richard Agbokpanzo
Electrical Engineering Department
University of Abomey-Calavi
Abomey-Calavi, Benin
richgille@gmail.com

Amevi Acakpovi
Electrical/Electronic Engineering Department
Accra Technical University
Accra, Ghana
acakpovia@gmail.com

2021 IEEE 8th International Conference on Adaptive Science and Technology (ICAST) | 978-1-6654-2717-3/21/$31.00 ©2021 IEEE | DOI: 10.1109/ICAST52759.2021.9682078

Abstract*—The aim of this study is to evaluate the magnetic field in the vicinity of the overhead high voltage transmission line, owing to the increasing concerns about the unpredictable health effects relating to magnetic field, produced by high voltage transmission lines. Low frequency magnetic fields around transmission line are time-varying quasi-static magnetic field for which the magnetic field is caused by current in the phase conductors. In this paper, the magnetic field produced by a power line is numerically modelled as the sum of the magnetic fields produced by each conductor current. Gmsh and GetDP open source software package are used for the simulation of the magnetic field created in the vicinity of two transmission lines that are located in Republic of Benin. The results of the study revealed that for the 161 kV and 330 kV transmission lines, there were some areas around the phase conductors where the magnitude of the magnetic field exceeded 75 μT and 200 μT respectively. A comparison of the study results with exposure limits specified by safety guidelines and regulations shows that there is no critical concern for the people living near the transmission lines. Rather, the exposure level seems dangerous for workers and individuals working closely to the line for a long duration. Consequently, the findings of this paper are useful in specifying appropriate clearance distance and duration to be maintain while working on life line as an amendment to existing standards in electromagnetic protection.

***Keywords*—HV transmission line, Magnetic Field, Electric Field, Electromagnetic Field, , Human Health, Electromagnetic compatibility,**

I. INTRODUCTION (*HEADING 1*)

Nowadays high voltage alternating current transmission lines are widely used for transmission of electrical energy for long distances. In the Republic of Benin, to ensure a smooth transmission of electricity to consumers, a wide area grid has been deployed. The national grid comprises a High voltage transmission system that uses the following voltages: 161 kV and 330 kV. As a direct consequence, magnetic and electric fields are induced in the vicinity of power line and in the neighboring environment. The question of whether exposure to extremely low-frequency magnetic fields (ELF-MFs) from power transmission is associated with an increased risk of childhood cancer has engendered scientific debate [1], [2]. In [3], ELF-MF is classified as "possibly carcinogenic to humans" (group 2B). The International Commission on Non-Ionizing Radiation Protection (ICNIRP) has assessed the available information on ELF-MF and has published in 2010, guidelines for limiting exposure to time-varying magnetic fields [4]. The Republic of Benin limits for emissions of magnetic field draw on the guidelines set by ICNIRP. The prescribed limits are to be four (4) times lower in areas that are more sensitive such as: living areas, schools and hospitals.

To reduce the aforementioned magnetic field emissions, different solutions have been attempted in the past. Some included: interchanging of phase sequences of line conductors; usage of very tall towers; optimal arrangements and placement of phase conductor determined by rigorous design principles.

Optimization process, has also been applied [5]-[7]. When magnetic field calculation is used in an optimization procedure, the computational effort required for the magnetic field calculation has an extremely important role. Overhead power line conductor sagging inside the span can be described by the catenary curve [6]-[7], which could require even higher computational efforts for accurate estimation of the magnetic field. In [8] George Filippopoulos developed the analytical formula of the magnetic field vector produced by power line for a single circuit line. The magnetic field produced by electric power lines is usually calculated analytically with the use of the Biot and Savart law. In [9], the magnetic field produced by power lines at relatively large distances in comparison to their phase spacing was analyzed. An analytical method for the evaluation of the emitted magnetic fields "far from the line" were presented. The model is very useful for the determination of the way the magnetic field decays as the distance increases. Furthermore, through this approach, it is not difficult to design a power line that produces a fast decaying magnetic field. Unfortunately, the analytical model is not very accurate close to the line, and thus they could not be used to determine the behavior of the magnetic field. In the current study the magnetic field produced by a power line is calculated in space 3D as the sum of the contribution of finitely small current elements of each phase conductor, a method very accurate at any distance,

978-1-6654-2717-3/21/$31.00 ©2021 IEEE

close to or far from the line. Gmsh and GetDP [10], [11] open source software package has been used for the simulation of the magnetic field created in the vicinity of the transmission lines, located in the Republic of Benin.

II. EASE GEOMETRIC AND CHARACTERISTICS

The specifications of the transmission lines were obtained from the Transmission Division of Republic of Benin's Energy Service Provider. The Figure1 shows the actual physicals of the overhead power lines. The Figure 2 shows the tower dimensions, the space arrangement and heights of the conductors of the power line in relation to the xyz axes system. That is a model of a power line with six phase conductors and one guard conductor. The line conductor are not straight, but they are sagged by their weight. The curve that is drawn by each conductor in a span between two sequential suspension points is known as the catenary. In order to simplify the calculations and the analysis of the magnetic field produced by the line, the model of an assembly of horizontal conductors parallel to the axis is used [11],[12]. This model is precise for the calculation of the magnetic fields if, as usual, the conductor sag is small in comparison to the span [13].

Figure 1 : Actual physical of conductors of the overhead power line for 161kV (a) and 330 kV (b)

Table 1 indicates the details of the voltage level and current capacity used in transmission lines.

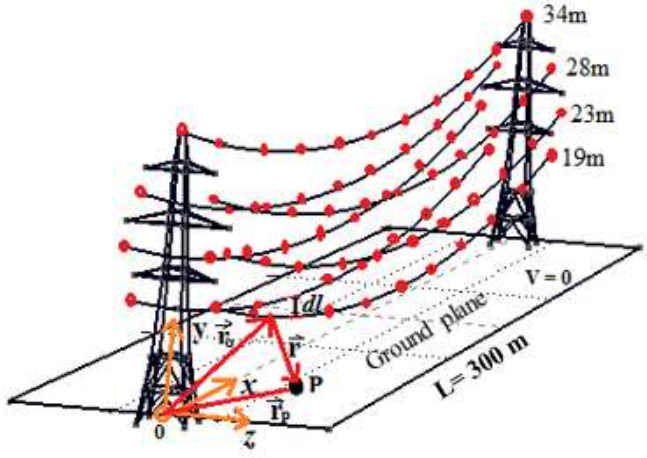

Figure 2: Positions of vectors $\vec{r}$, $\vec{r}_0$ and $\vec{r}_p$ in relation to the observer *P*

On figure 2, P is any desired point of calculation in space of $\vec{B}$; $\vec{\mathbf{r}}$ is vector points from element of conductor *dl* to P ; $\vec{\mathrm{r}}_\mathrm{p}$ vector points from origin of coordinate system to *P* and $\vec{\mathrm{r}}_0$ points from origin of coordinate system to element of conductor *dl*

I is current in phase conductor, dl is element of length along the path taken by the current,

$\vec{\mathbf{r}}$ can be written as follows : $\vec{\mathbf{r}} = \vec{\mathrm{r}}_\mathrm{p} - \vec{\mathrm{r}}_0$ (1)

Table 1 *: Details of the transmission lines*

Voltage level (kV)	161 kV	330 kV
Current each conductor(A)	485 A	1700 A

III. MAGNETIC FIELD CALCULATION

For a overhead power line with complex shapes of conductors as a catenary, it is necessary to use a numerical method to calculate magnetic field. Application of this method for every conductor shape, means the change from analytic form consisting of unit derivations to numerical form consisting of unit differences. This can be applied for électric and magnetic fields components.

The magnetic flux density produced by the power line at any point in space can be represented using vectors and phasors. A magnetic flux density vector is characterized by three spacial components [14]

$$\vec{B} = [B_x; B_y; B_z] \quad (2)$$

and Phasor represents the quantity with a sinusoidal time variation described by a magnitude and a phase angle. Angle φ_x describes phase shift [15].

$$B_x(t) = B_x e^{j\varphi_x} e^{j\omega t} \quad (3)$$

Three orthogonal components of vector may be phasors with different magnitude and phase angles. This components are called phase–vector (Equation 4) [16].

$$\hat{\vec{B}} = [\hat{B}_x; \hat{B}_y; \hat{B}_z] \quad (4)$$

For calculation of $\hat{\vec{B}}$ it is desired to know :

- geometry of the system, position of phase conductors and guard wires in 3D space,
- currents of phase conductors,
- position of the point of observer P.

The calculation consists of two steps: the calculation of the line currents and the calculation of the produced field. In this study, the line currents are assumed to be balanced without higher harmonic components. The effects of the ground induced currents and of the varying electric field on the total magnetic field are considered negligible [17], [18].

Calculation of the $\hat{\vec{B}}$ is based on summation of the contribution of finitely small elements of each phase conductor into single point of observer P. Calculation can be described by these following steps:

- differentiation of conductors into elements of finite length.
- enumeration of $\hat{\vec{B}}$ in single point of observer as a result of summing the contribution to the field from all element.

Starting from Biot–Savart law, which can be derived from Ampere-Laplace equations with a quasi-static assumption, as follows:

$$\vec{B} = \frac{\mu_0}{4\pi}\int_l \frac{I\vec{dl}\times\vec{r}}{r^3} \quad (5)$$

Where μ_0 is air magnetic permeability constant ($4\pi 10^{-7}$H/m).

The vector $\vec{r}$ can be replaced by a difference of vectors $\vec{r}_0$ and $\vec{r}_p$ as shown in figure 2.

Equation can be rewritten as follows:

$$d\vec{B} = \frac{\mu_0}{4\pi}\frac{Id\vec{l}\times(\vec{r}_p-\vec{r}_0)}{\left|(\vec{r}_p-\vec{r}_0)^3\right|} \quad (6)$$

The Equation 6 along the catenary shape of conductor, the method based on numeric integration, can be used. The conductor is split into a finite number of small elements with length $d\vec{l}_k$. Integral along catenary curve is approximated by summation of contributions $d\vec{B}_k$ created by finite elements k of the conductor.

Introducing sinusoidal varying current of the conductor k = 1, 2, … is represented by its phasor $\hat{I}_k$. In the classical space vector representation, the magnetic flux density $\vec{B}_k$, created by finite elements k of the conductor.

can be written

$$\hat{\vec{B}}_k = \frac{\mu_0}{4\pi}\sum_{k=1}^{k}\frac{\hat{I}_k d\vec{l}\times(\vec{r}_p-\vec{r}_{0k})}{\left|(\vec{r}_p-\vec{r}_{0k})^3\right|} \quad (7)$$

If n is the number of phase conductors of the overhead power line, in our case(n = 6). Using the superposition theorem, the magnetic flux density $\hat{\vec{B}}$ produced by the line is the sum of the fields produced by each conductor separately

$$\hat{\vec{B}} = \frac{\mu_0}{4\pi}\sum_{n=1}^{n}\left[\sum_{k=1}^{k}\frac{\hat{I}_k d\vec{l}\times(\vec{r}_p-\vec{r}_{0_{kn}})}{\left|(\vec{r}_p-\vec{r}_{0_{kn}})^3\right|}\right] \quad (8)$$

The magnetic flux density vector occurred in (8) with its classical representation as is described in [12]. That is a vector in the 3D space xyz whose components in each axis is sinusoidal varying with time.

If :

$$\hat{\vec{B}}_x = \hat{\vec{B}}_{xr} + j\hat{\vec{B}}_{xi}\ ; \quad (9)$$

$$\hat{\vec{B}}_y = \hat{\vec{B}}_{yr} + j\hat{\vec{B}}_{yi}\ ; \quad (10)$$

$$\hat{\vec{B}}_z = \hat{\vec{B}}_{zr} + j\hat{\vec{B}}_{zi}\ ; \quad (11)$$

are the components of the magnetic field in x, y and z axis, respectively, then the vector $\hat{\vec{B}}$ is written as :

$$\hat{\vec{B}} = \hat{B}_x\hat{\mathbf{e}}_x + \hat{B}_y\hat{\mathbf{e}}_y + \hat{B}_z\hat{\mathbf{e}}_z \quad (12)$$

$$= \hat{B}_r + j\hat{B}_i \quad (13)$$

$$\hat{\vec{B}} = B_{xr}\hat{\mathbf{e}}_x + B_{yr}\hat{\mathbf{e}}_y + B_{zr}\hat{\mathbf{e}}_z + jB_{xi}\hat{\mathbf{e}}_x + jB_{yi}\hat{\mathbf{e}}_y + jB_{zi}\hat{\mathbf{e}}_z \quad (14)$$

where $\hat{\mathbf{e}}_x$, $\hat{\mathbf{e}}_y$ and $\hat{\mathbf{e}}_z$ are the unit vectors on x, y and z axis, respectively, and the vectors $\vec{B}_r = B_{xr}\hat{\mathbf{e}}_x + B_{yr}\hat{\mathbf{e}}_y + B_{zr}\hat{\mathbf{e}}_z$ and $\vec{B}_i = B_{xi}\hat{\mathbf{e}}_x + B_{yi}\hat{\mathbf{e}}_y + B_{zi}\hat{\mathbf{e}}_z$ are the real and imaginary part of $\hat{\vec{B}}$, which corresponds to the real and the imaginary part $I_{k,r}$ and $I_{k,i}$, respectively, of the currents $\underline{I}_k = I_{k,r} + jI_{k,i}$.

For the Magnetic field calculation, the equation (8) has been used and solved with GetDP tools.

The magnitude of the magnetic field is usually characterized by its resultant rms value, which is equal to

$$B = \sqrt{(B_x^2 + B_y^2 + B_z^2} = \sqrt{(B_r^2 + B_i^2} \quad (15)$$

$$= \sqrt{(B_{xr}^2 + B_{yr}^2 + B_{zr}^2 + B_{xi}^2 + B_{yi}^2 + B_{zi}^2} \quad (16)$$

This parameter is generally used to determine the magnitude of the magnetic field in order to compare it with exposure limits.

IV. Boundary Conditions

For magnetic problem, some Dirichlet conditions have been used. Dirichlet conditions are electric current in boundary of phase conductors sections. The electric current on phase conductors sections of the power line is as follows

$$\hat{I}_{1a} = I\,, \hat{I}_{1b} = Ie^{-j2\pi/3}\,, \hat{I}_{1c} = Ie^{-j4\pi/3} \quad (17)$$

$$\hat{I}_{2a} = Ie^{-j4\pi/3}, \hat{I}_{2b} = Ie^{-j2\pi/3}, \hat{I}_{2c} = I \quad (18)$$

The different parts of the overhead high voltage line such as the pylon, the phase and guard conductors positions, are modelled using the open source mesh generator Gmsh (Dular et al. 1998). This is a 3D finite elements grid generator with build-in CAD system. The magnetic field calculations are performed using the multi-physics finite element solver GetDP (Geuzaine & Remacle 2009). Gmsh and GetDP are integrated in the graphical environment.

In end, matlab software are used to treat data and plot the graphes.

V. Results and Discussion

A proposed numerical method for the determination of the magnetic field vector in the vicinity of any arbitrary power line has been used for the simulation of magnetic field in the vicinity of the 161kV and 330 kV transmission lines. Part A of this section cover simulation results for 161kV and Part B cover simulation results for 330 kV. The transmission line phase conductors, which represent sources, are oriented along the x-axis in the global Cartesian coordinate system (x, y, z). The calculation of the magnetic field was carried out in the horizontal x-z plane and vertical y-z plane. The y-z plane is perpendicular to the observed transmission line section. Gmsh

and GetDP open source software package are used for analysis.

A. 161 kV Transmission Line

Simulation results in the Figure 3 show the shapes of the magnetic field distribution in the x-z plane below the overhead transmission lines at a height 1.5 m above the earth. Figure 4 show the lateral magnetic field profile as a function of the distances. The maximum value of the magnetic field is found in the middle of the span field at the co-ordinates x = 150 m. The maximum value of the magnetic field strength is 11.6 µT. Moving away from phases conductors, the magnetic field decrease and was then less important in both directions. The maximal fields produced show that the limits given in Table 2 are not exceeded based on the current configuration.

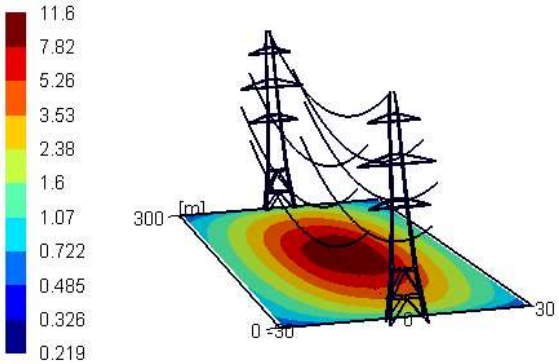

Figure 3 : Magnetic Field Distribution (µT) in *x-z* Plane at 1.5m above the earth, for 161kV Carry out by Gmsh

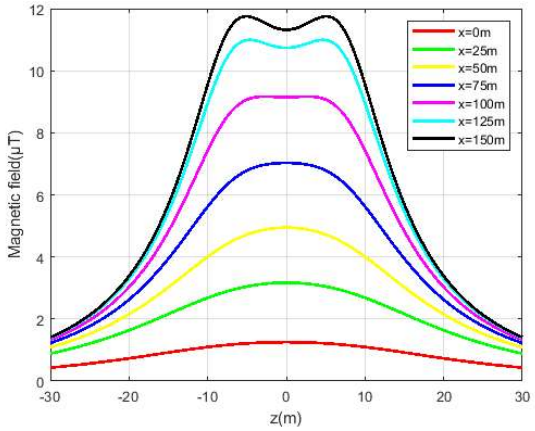

Figure 4 : Lateral magnetic field (µT) profile calculated at 1.5m above the earth for 161kV for different distance along of the line

Figure 5 shows the shapes of the magnetic field distribution in the y-z plane. Magnetic field strength increases and becomes stronger near the phase conductors (with Bmax = 75µT). In Figure 6, the lateral magnetic field profile is calculated at mid-span length for different heigh above the earth. Here, the values of the magnetic field strength increase with the height increases and reached the maximum values near the phase conductors. When moving away from the z-axis with a distance z = ±30 m, the values of the magnetic field reduces. Thus, a decrease was observed according to the distance. Referring to Table 2, the values of the magnetic field are far below the maximum allowed exposure values for the general public.

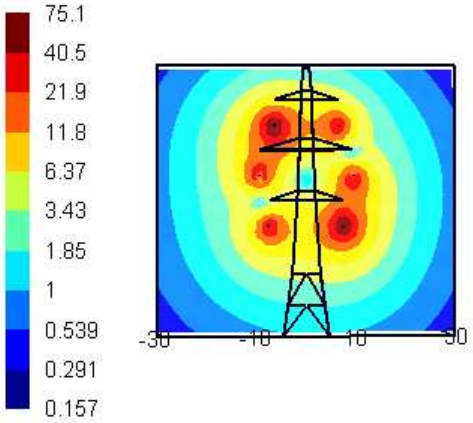

Figure 5 : Magnetic field (µT) distribution in the y-z plane for 161kV transmission line, Carry out by Gmsh (b)

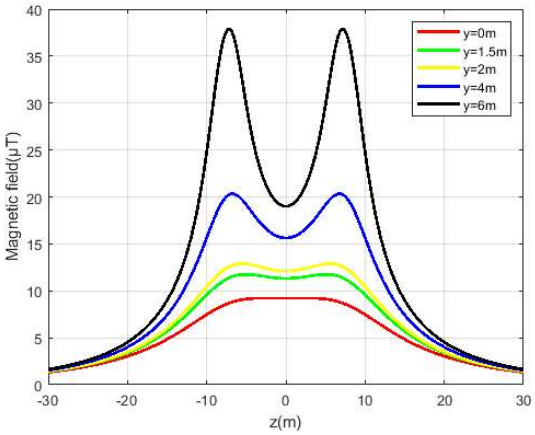

Figure 6: Lateral magnetic field (µT) profile calculated at mid-span length for different heigh above the earth for 161kV transmission line

B. 330 kV Transmission Line

The simulation results in Figure 7 show the shapes of the magnetic field distribution in the x-z plane below the overhead transmission lines at a height 1.5 m above the earth. The Figure displays the magnetic field as a function of the distances. The maximum value of the magnetic field is found in the middle of the span field at the co-ordinates x = 150 m. The maximum value of the magnetic field strength is 40.8 µT, thus below the maximum allowed exposure values for the general public given by the standard specification in Table 2.

Moving away from phases conductors, the magnetic field decrease and is less significant in both directions. The figure 8 shows the distribution of the magnetic field in the y-z plane. Magnetic field strength increases and takes a strong value near the phase conductors (with Bmax = 263µT). In Figure 9, magnetic field is plotted, at the middle of the span field at the co-ordinates x = 150 m, up to some distance from ground surface and it is repeated for various heights from the ground surface and respective heights of 1.5m, 2m, 4m, 6m above the ground surface. Here, the values of the magnetic field strength increases while the height increases and reach the maximum values near the phase conductors (with Bmax = 135µT). Referring to Table 2, the maximum values of the magnetic field are far above the maximum allowed exposure values for the general public given by the standard specifications in

Table 2. When moving away from the z-axis with a distance z = ±30 m, the values of the magnetic field are completely low and insignificant. Consequently, a decrease is observed according to the distance.

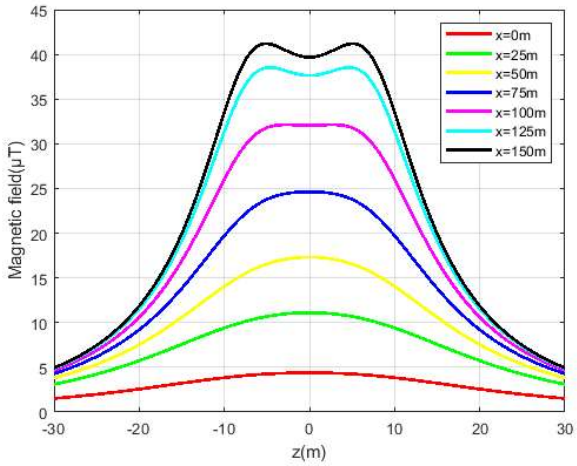

Figure 7: Lateral magnetic field (μT) profile calculated at 1.5m above the earth for different distance along of the 330 kV transmission line

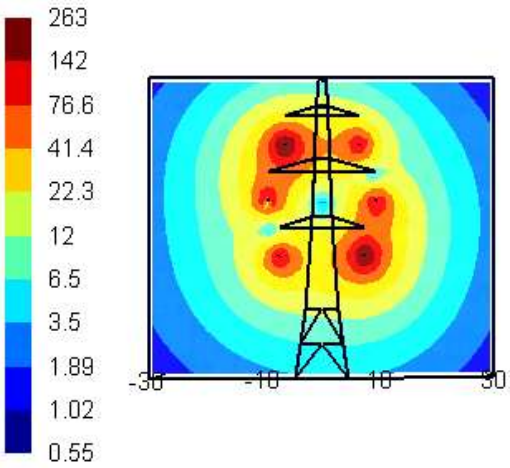

Figure 8: Magnetic field (μT) distribution in the y-z plane for 330kV transmission line, Carry out by Gmsh (b)

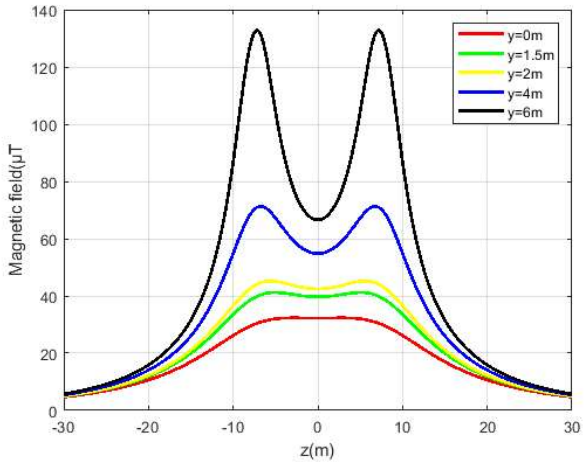

Figure 9: Lateral magnetic field (μT) profile calculated at mid-span length for different heigh above the earth for 330kV transmission line

Table 2 : Limitation exposure to low frequency electric and magnetic fields (50 Hz) ICNIRP (2010)

Power lines (50Hz)		
	Electric field	Magnetic field
Professional exposure limits 8h/j	10kV/m	100 μT
Residential exposure limits 24h/24h	5kV/m	200 μT

VI. CONCLUSION

In summary, this study adopted an numerical intégration method of calculating the magnetic field vector in the vicinity of any arbitrary power line effectively. The application of the model was made possible through the representation of the magnetic field vectors phasors. The model gave accurate and valid output irrespective of the distance. Simulation results revealed that there are some areas in the vicinity of the overhead high voltage transmission lines where the magnetic field intensity has exceeded the maximum allowed exposure values for the general public or workers, according to standard specifications. However the magnetic field decreases based on distance from source to field point. Besides, magnetic field is produced based on current flowing in the phase conductor. Also, load demands influences the magnetic field values. Finally, this paper clarifies the myth or misunderstanding about health effects of overhead transmission lines especially for people living in close vicinity.

ACKNOWLEDGMENT

The authors gratefully acknowledge the reviewers of this paper for their valuable advice and guidance. Thanks to Christophe Geuzaine, Electrical engineering department, University of Liege, Belgium for the support to the authors.

REFERENCES

[1] Kheifets L. Ahlom A. Crespi CM, draper G. Hagihara J. Lowenthal RM, et al. "Pooled analysis of extremely low-frequency magnetic fields and childhood braintumors, ". Am J Epidemiol.2010 ; 172 (7) :752-61. Epub 2010/08/11. https://doi.org/10.1093/aje/kwg181 PMD : 20696650 : PubMed Central PMCID : PMC2984256

[2] [2] Kheifets L. Ahlom A. Crespi CM, draper G. Hagihara J. Lowenthal RM, et al. "Pooled analysis of recent studies on magnetic fields and childhood leukaemia," Br J cancer 2010 ; 103(7) :1128-35. Epub2010/09/30. https://doi.org/10.1038/sj.bjc.6605838 PMID : 20877339 ; PubMed central PMCID : PMC2865855

[3] IARC, "Non-ionizing radiation, Part 1 : Static and extremely low-frequency (ELF) electric and magnetic fields, IARC Monographs on the Evaluation of Carcinogenic Risks to Humans, Vol. 80, 1–395, 2002.

[4] International Commission on Non-ionizing Radiation Protection, "Guidelines for limiting exposure to time-varying electric and magnetic fields (1Hz to 100 kHz)," Health Physics, Vol. 99, No. 6, 818–836, 2010.

[5] H. Ahmadi, S. Mohseni, A. A. Shayegani Akmal "Electromagnetic fields near transmission lines – problems and solutions" *Iran. J. Environ. Health. Sci. Eng., 2010, Vol. 7, No. 2, pp. 181-188*

[6] K. Deželak, G. Štumberger, F. Jakl, "Emissions of Electromagnetic Fields caused by Sagged Overhead Power Lines," Przeglad Elektrotechniczny, 2011, vol. 87, no. 3, pp. 29-33

[7] W. T. Kaune and L. E. Zaffanella, "Analysis of magnetic fields produced far from electric power lines," *IEEE Trans. Power Del.*, vol. 7, no. 4, pp. 2082–2091, Oct. 1992.

[8] G. Filippopoulos and D. Tsanakas, IEEE Trans. Power Del. 20, 1474 (2005).

[9] A. Tzinevrakis, D. Tsanakas, E. Mimos "Analytical calculation of the electric field produced by single circuit power lines with horizontal arrangement of the conductors" 51st International Scientific Colloquium,Technische Universität Ilmenau September 11 – 15, 2006

[10] Dular P., Geuzaine C., Henrotte F. and Legros W., "A General Environment for the Treatment of Discrete Problems and its Application to the Finite Element Method", IEEE Transactions on Magnetics, 34(5), pp. 3395 3398, 1998.

[11] Geuzaine C. and Remacle J.-F., "Gmsh, a three-dimensional finite element mesh generator with built-in pre- and post-processing facilities", International Journal for Numerical Methods in Engineering 79(11), 1309-1331, 2009.

[12] D.W. Deno and L. E. Zaffanella, "Field effects of overhead transmission lines and stations," in Transmission Line Reference Book—345 kV and Above, 2nd ed, CA : Elect. Power Res. Inst., 1982, ch. 8.

[13] A. V. Mamishev, R. D. Nevels, and B. D. Rushell, "Effects of conductorsag on spatial distribution of power line magnetic field," *IEEE Trans. Power Del.*, vol. 11, no. 3, pp. 1571–1576, Jul. 1996.

[14] M. Cessenat, Mathematical methods in electromagnetism, ser. Series on Advances in Mathematics for Applied Sciences. River Edge, NJ: World Scientific Publishing Co. Inc., 1996, vol. 41, linear theory and applications.

[15] EPRI, AC transmission line reference book - 200 kV and above, 3rd ed.Electric Power Research Institute, 2005.

[16] EPRI, AC Transmission Line Reference Book – 345 kV and above, 2nd ed. Electric Power Research Institute, 1982.

[17] R. G. Olsen and T. A. Pankaskie, "On the exact, Carson and image theories for wires at or above the earth's interface," IEEE Trans. Power App. Syst., vol. PAS-102, no. 4, pp. 769–778, Apr. 1983.

[18] R. G. Olsen and P. S. Wong, "Characteristics of low frequency electric and magnetic fields in the vicinity of electric power lines," IEEE Trans. Power Del., vol. 7, no. 4, pp. 2046–2055, Oct. 1992.